

# A NUMERICAL INVESTIGATION OF THE AIR-SEA INTERACTION AT THE COASTAL UPWELLING AREA OF CABO FRIO USING COUPLED MODELS

*Flávia Noronha Dutra Ribeiro<sup>1</sup>, Jacyra Soares<sup>2</sup>, Amauri Pereira de Oliveira<sup>3</sup>.*

<sup>1</sup> Aluna de doutorado do IAG-USP, Rua do Matão, 1226, São Paulo, SP, tel.: 3091-2851, fax: 3091-4714, fndutra@model.iag.usp.br

<sup>2</sup> Professora Doutora do IAG-USP, tel.: 3091-4711, fax: 3091-4711, jacyra@usp.br

<sup>3</sup> Professor associado do IAG-USP, tel 3091-4701, apdolive@usp.br

**RESUMO:** Um modelo numérico oceânico de 1 ½ camada é desenvolvido para ser acoplado ao modelo atmosférico TVM-NH para estudar a influência da temperatura da superfície do mar na camada limite planetária da área de ressurgência costeira de Cabo Frio (RJ, Brasil). O modelo oceânico é de diferenças finitas e tem uma camada superficial, que usa a versão turbulenta das equações de momento, continuidade e calor, e uma camada profunda que é inerte. Foram realizados experimentos numéricos usando uma linha de costa idealizada para validar as condições de fronteira e um experimento usando uma linha de costa realística. O acoplamento é proposto e testado, e os resultados são comparados à imagem de satélite. Os resultados mostram que o modelo é capaz de representar muito bem o fenômeno de ressurgência costeira em Cabo Frio e pode ser eficientemente acoplado ao modelo atmosférico TVM-NH.

**ABSTRACT:** An 1 ½ layer oceanic numeric model is developed to be coupled to the Topographic Vorticity-mode Mesoscale- Non Hydrostatic (TVM-NH) atmospheric model to study the influence of the sea surface temperature (SST) on the planetary boundary layer (PBL) of the coastal upwelling area of Cabo Frio (RJ, Brazil). The oceanic model is finite differenced and has an upper layer that uses the turbulent version of the momentum, continuity and heat equations and an inert deep layer. Numerical experiments were performed using an idealized coastline to validate the boundary conditions and then using a realistic coastline. The coupling is proposed and tested, and the results are compared to the satellite image. Results show that the model is capable of representing fairly well the coastal upwelling phenomenon at Cabo Frio and it is suitable for coupling with the atmospheric model TVM-NH.

**Palavras-Chave:** coupled oceanic-atmospheric model, coastal upwelling,

## INTRODUCTION

The southeast coast of Brazil (21° to 27°S, 40° to 47°W) very often presents the phenomenon of coastal upwelling due mainly to the presence of a large scale high pressure center over the South Atlantic Ocean. This center generates northeasterly surface winds over the coast, which are favorable to the development of the coastal upwelling, since it causes Ekman transport of the surface water away from the coast, allowing deeper and colder water to surface. Therefore, the upwelling is characterized by cold anomalies of SST. With the passage of cold fronts, the wind direction changes counterclockwise, blowing from the Southwest. Southwesterly winds are unfavorable to the coastal upwelling at Cabo Frio and cause the SST to increase.

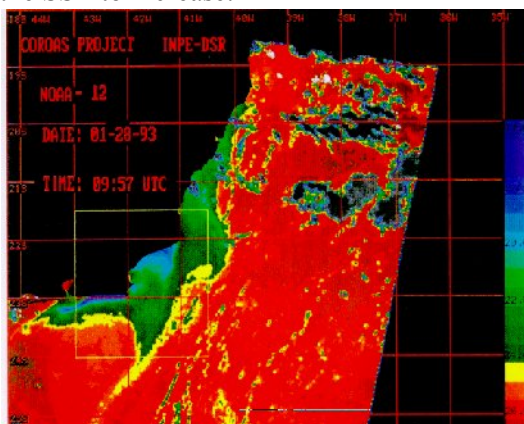


Figure 1: Satellite image of the SST field at the Brazilian Southeast coast. The yellow square represents the investigated region of this work.

Figure 1 shows a satellite image of the SST field at the coast of Brazil. The yellow rectangle points the area of Rio de Janeiro (RJ), where are two capes: Cabo Frio (23°S, 42°W) and Cabo de São Tomé (22°S, 41°W). At west of both capes, there are areas of cold water, but Cabo Frio has a longer area near the coast with very low SST.

Coastal upwelling is a very important phenomenon at Cabo Frio because it brings nutrient rich water to the coast and improves the fishery activities. The colder SST also has an impact on atmospheric processes and weather conditions, but only a few works have investigated this interaction at this area. Franchito *et. al* (1998) used an atmospheric model forced by oceanic data and a oceanic model forced by atmospheric data and suggested that there is a positive feedback between the coastal upwelling and the sea breeze at Cabo Frio.

Oda (1997) performed radiosonde soundings to evaluate the depth of the planetary boundary layer and observed that the PBL is more stable during the occurrence of upwelling. Dourado and Oliveira (2001)

investigated through observational data, taken during the passage of a cold front in 1992, the evolution of the vertical extent of the atmospheric and the oceanic boundary layers at Cabo Frio. It was observed a depth growth of both boundary layers caused by the warmer SST and by stronger winds. Later on, they used a one-dimension atmospheric second order closure model coupled to an oceanic mixed layer model to investigate the short term variation of the atmospheric and oceanic boundary layers at Cabo Frio, taking as reference the observations gathered before (Dourado and Oliveira, 2008). The model results indicated that the thermal contrast is not strong enough to generate oceanic and an atmospheric boundary layers as deep as observed.

The atmospheric TVM-NH (Topographic Vorticity-mode Mesoscale - Non Hydrostatic) model was successfully used by researchers at coastal areas to investigate mesoscale atmospheric processes such as sea breeze (Clappier *et. al*, 2000; Orgaz and Fortes, 1998) and lake breeze (Stivari *et al.* 2003).

The objective of this work is to develop an oceanic model capable of representing the coastal upwelling phenomenon and suitable for coupling with the TVM-NH atmospheric model to study the interaction between ocean and atmosphere during an upwelling event at Cabo Frio.

## NUMERICAL MODELS

**Oceanic numerical model:** The model is based on the one described by Carbonel (2003). It has a lower layer with constant temperature and no pressure gradients and an upper layer where the governing equations are the vertically-integrated non-linear equations of momentum, continuity and transport of SST, as follows:

$$\frac{\partial U}{\partial t} + \frac{\partial uU}{\partial x} + \frac{\partial vU}{\partial y} - fV + gh \left\{ \sigma \frac{\partial h}{\partial x} + \frac{h\theta}{2\mu} \frac{\partial T}{\partial x} \right\} + rU - \frac{\tau_x}{\rho^u} = 0 \quad (1) \quad \frac{\partial h}{\partial t} + \frac{\partial U}{\partial x} + \frac{\partial V}{\partial y} - w_e = 0 \quad (3)$$

$$\frac{\partial V}{\partial t} + \frac{\partial uV}{\partial x} + \frac{\partial vV}{\partial y} + fU + gh \left\{ \sigma \frac{\partial h}{\partial y} + \frac{h\theta}{2\mu} \frac{\partial T}{\partial y} \right\} + rV - \frac{\tau_y}{\rho^u} = 0 \quad (2) \quad \frac{\partial T}{\partial t} + u \frac{\partial T}{\partial x} + v \frac{\partial T}{\partial y} + \frac{1}{h} (q - Q) = 0 \quad (4)$$

where U and V are the transport components ( $U = hu; V = hv$ ) in the x and y direction respectively, u and v are the velocity components,  $f$  is the Coriolis parameter;  $g$  is the gravity acceleration,  $h$  is the upper layer thickness,  $T$  is the SST,  $\tau_x(\tau_y)$  is the component of the wind stress at the x (y) direction defined as

$\tau_i = \rho^{air} C_D w_i |W|$   $i=x,y$ ,  $\rho^{air}$  is the air density,  $C_D$  is the drag coefficient,  $W$  is the wind velocity intensity,  $r$  is the Rayleigh friction coefficient,  $w_e$  is the entrainment velocity defined as  $w_e = \frac{(H-h)^2}{t_e H}$  when  $h \leq H_e$  and

$w_e = 0$  otherwise,  $H_e$  is the entrainment thickness,  $t_e$  is the entrainment time scale,  $H$  is the initial upper layer thickness,  $q$  is the source or sink of heat across the interface defined as  $q = H \frac{\partial U}{\partial x} \left( \frac{T - T^l}{h} \right) + H \frac{\partial V}{\partial y} \left( \frac{T - T^l}{h} \right)$ ,

$T^l$  is the initial temperature of the inert layer,  $Q$  is the surface heat flux, defined as  $Q = \frac{H^2}{t_s} \left( \frac{T^u - T}{h} \right)$ ,  $T^u$  is the

initial temperature of the upper layer,  $t_s$  is the surface heat flux time scale,  $\rho^u$  is the upper layer density,

$\rho^l$  is the inert layer density,  $\theta$  is the thermal expansion coefficient,  $\sigma$  and  $\bar{\mu}$  are density coefficients defined

as  $\bar{\mu} = \frac{\mu}{(\mu - \sigma)}$ ,  $\mu = \frac{\rho^u}{\rho^l}$  and  $\sigma = 1 - \mu$ .

The boundaries are of two types: land and ocean. At land type boundary, the velocity and transport components normal to the boundary are set to zero and  $h$  and  $T$  are assumed homogeneous. At ocean type boundary, the weakly-reflective boundary condition described by Verboom and Slob (1984) is used. It is based on the characteristic method and it is applied on an axis normal to the boundary ( $n$ ), as follows:

$$\frac{\partial (U_n \pm ch)}{\partial t} + c \frac{\partial (U_n \pm ch)}{\partial x_n} \pm c (w_e) + \frac{\partial (u_n U_n)}{\partial x_n} + \varepsilon_n + \frac{gh^2 \theta}{2\mu} \frac{\partial T}{\partial x_n} - \frac{\tau_n}{\rho^u} + rU_n = 0 \quad (5)$$

where  $c = \sqrt{\sigma gh}$  is the characteristic velocity.

The order of calculation is: first the heat exchanges  $q$  and  $Q$  are calculated; next the SST ( $T$ ); then the pressure ( $p$ ); after that, the transport components  $U$  and  $V$  and at last, the thickness of the active layer  $h$ . The current components are then obtained by the division of the transport components by the thickness  $h$ . The constant parameter values are the same used by Carbonel (2003).

**Atmospheric numerical model:** The non-hydrostatic version of the TVM model, developed by Thunis (1995), is three-dimensional, follows the Boussinesq approximations of the vorticity equations, obtained

from the basic Reynolds-averaged equations, of motion and uses sigma coordinates. The vorticity approach makes the pressure and the density variables to drop out from the equations.

The vertical grid is structured as follows: soil parameters at the bottom boundary; the first layer is the surface boundary layer, where the meteorological parameters are obtained by similarity theory equations; and the other layers are governed by the finite approximation of the hydrodynamic and thermodynamic equations.

The soil parameters are determined in the following order: first the model evaluates solar and infrared radiative fluxes and calculates the net radiation  $R_N$ ; then it obtains the soil heat flux  $G$  by

$$G = R_N - H - LE \quad (6)$$

where  $H$  is the sensible heat flux and  $LE$  is the latent heat flux from previous time step; at last the surface temperature is computed for all soil types except water by the force-restore method of Deardorff (1978), and specific humidity is computed using the Penmann-Monteith method. For water, the temperature is constant.

The surface boundary layer fluxes are then evaluated by

$$\tau = -\rho_0 u_*^2 \quad H = -\rho_0 C_p u_* \theta_* \quad E = -\rho_0 L_v u_* q_* \quad (7)$$

where  $\tau$  is the wind stress,  $\rho_0$  is the density of air,  $C_p$  is the specific heat at constant pressure,  $L_v$  is latent heat of water vaporization,  $u_*$  is the velocity scaling parameter,  $\theta_*$  is the potential temperature scaling parameter and  $q_*$  is the specific humidity scaling parameter. The fluxes values are then used to force the hydrodynamic and thermodynamic equations at the other layers of the domain, time is advanced and the cycle is repeated. For a more detailed description of the model, see Thunis (1995).

**Coupling between the oceanic and atmospheric model:** The oceanic model was developed in the form of a subroutine and set to use the same horizontal grid spacing as the TVM-NH model. When the atmospheric model starts, it calls the oceanic model subroutine that returns a 2 days integration SST field. Then the SST field is used by the TVM-NH model to determine the surface heat flux over the ocean. The time step of the TVM-NH and the oceanic models are, respectively, 30 and 600 seconds. Therefore, the SST field remains the same for 20 time steps of the TVM-NH, and then the oceanic model is called again. The TVM-NH model forces the oceanic model with the wind stress obtained by equation (7) and the surface soil heat flux obtained by the equation (6). The oceanic model then updates the SST field and returns to the TVM-NH model.

## RESULTS

**Validation of the oceanic boundary condition:** Numerical experiments, hereafter called boundary experiments, were performed to validate the oceanic boundary condition by forcing the model with constant winds of  $8 \text{ ms}^{-1}$  from NE and SW. The area of the domain has  $180 \times 180 \text{ km}$  using 101 grid points in both directions. At each case, a reference experiment was performed with a larger area ( $360 \times 360 \text{ km}$  and 201 grid points) to investigate the boundary influence on the central area of the domain.

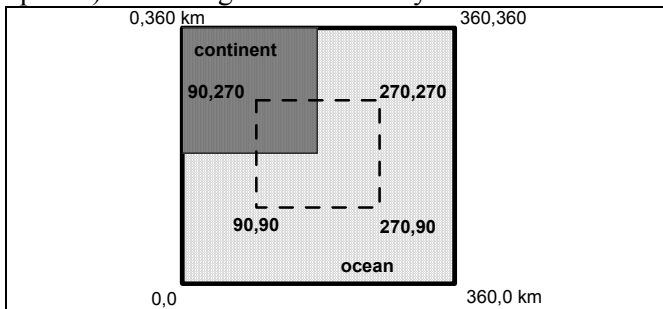


Figure 2: Scheme of the reference domain experiment. The area delimited by the dashed line is the domain used to compare to the boundary experiments.

The central area of the reference experiment is compared to the total area of the boundary experiment (Fig. 2). Figures 3 and 4 show the resulting SST fields after 4 days of integration for the boundary experiments on the left (a) and for the reference experiments on the right (b). The boundary experiments show the influence of the boundary at the SST values near the boundary but the difference between them and the reference experiments is never greater than  $0.5^\circ\text{C}$ . At the central area, the difference is even smaller.

Since that the duration time of integration was greater than it is needed for the coupled experiment and the analyzed area is the central area, the boundaries proved to be very weakly-reflective and the results are found satisfying. The results show also the expected response of the SST at each wind forcing. Figure 3 corresponds to the northeasterly wind forcing. The wind stress component parallel to the left part of the domain has the coast on its right side, and, in the Southern Hemisphere, it forces the Ekman transport away from the coast causing coastal upwelling and cold SST anomalies.

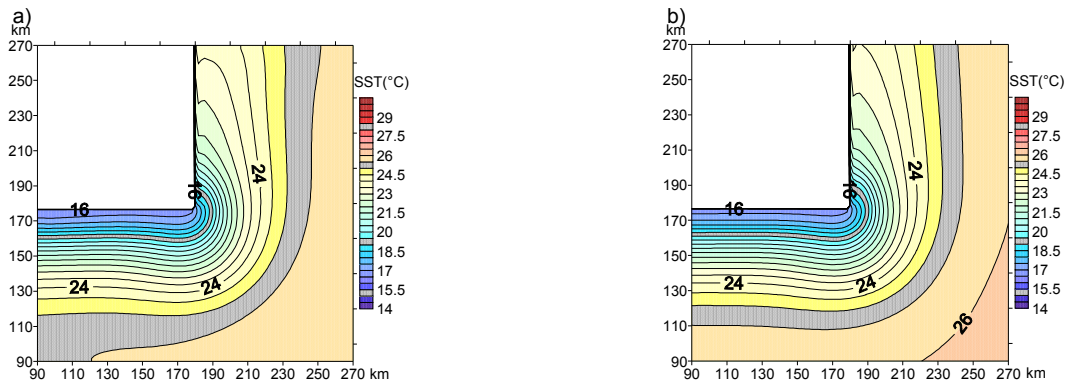


Figure 3: SST field after 4 days forced by constant northeasterly winds in the (a) small domain and (b) reference domain.

Figure 4 corresponds to the southwesterly wind forcing that has the opposite effect as the northeasterly wind and causes downwelling and warm SST anomalies.

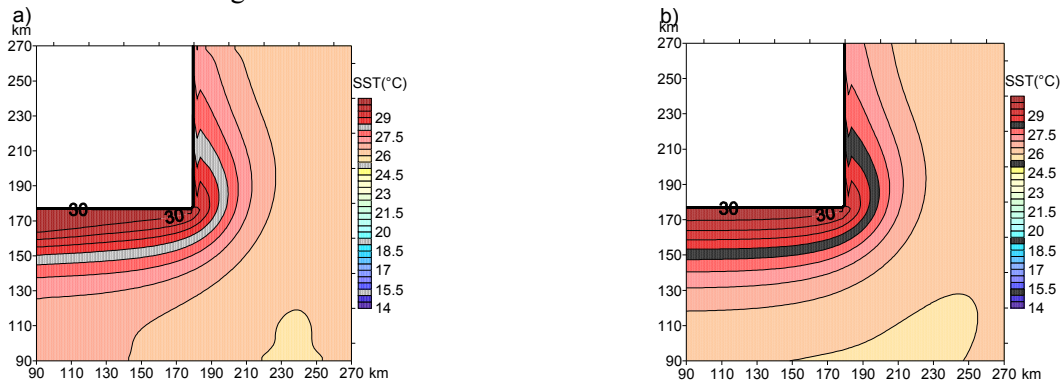


Figure 4: SST field after 4 days forced by constant southwesterly winds in the (a) small domain and (b) reference domain.

**Validation of the spatial distribution of SST:** A numerical experiment using a realistic coastline is performed. The domain used is 218x218 km representing the area from 21.8°S to 22.78°S and 41°W to 43.05°W (Fig. 5). The grid spacing is 3km at a central area of 100x100km and increases with a geometric progression with a ratio of 1.2 toward each boundary. This grid spacing was chosen to match the one used by the atmospheric model TVM-NH. The forcing is a constant northeasterly wind with  $9 \text{ ms}^{-1}$  of intensity.

Figure 6 shows the SST field generated by the oceanic model after 2 days of integration. It shows that the upwelling is stronger just west of the cape, where the coastline is E-W and the wind component parallel to the coast is strong. With the change of the direction of the coastline to N-S, the SST is warmer, because the strongest wind component is normal to the coastline. At the upper right part of the domain, the SST drops again, since the wind is mainly parallel to the coast.

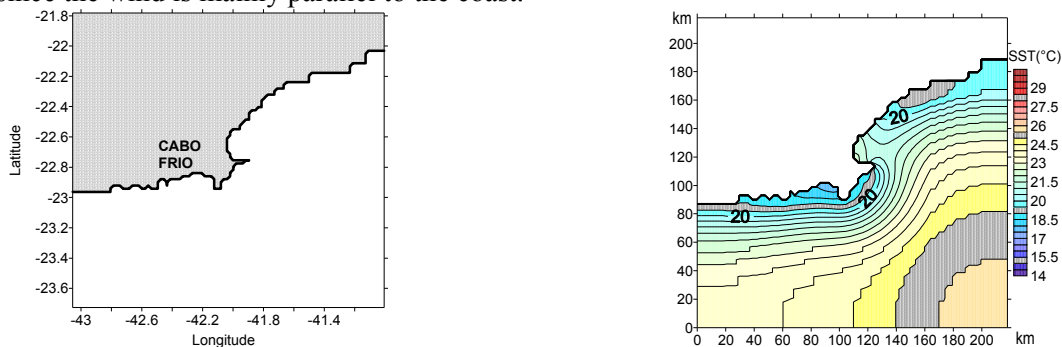
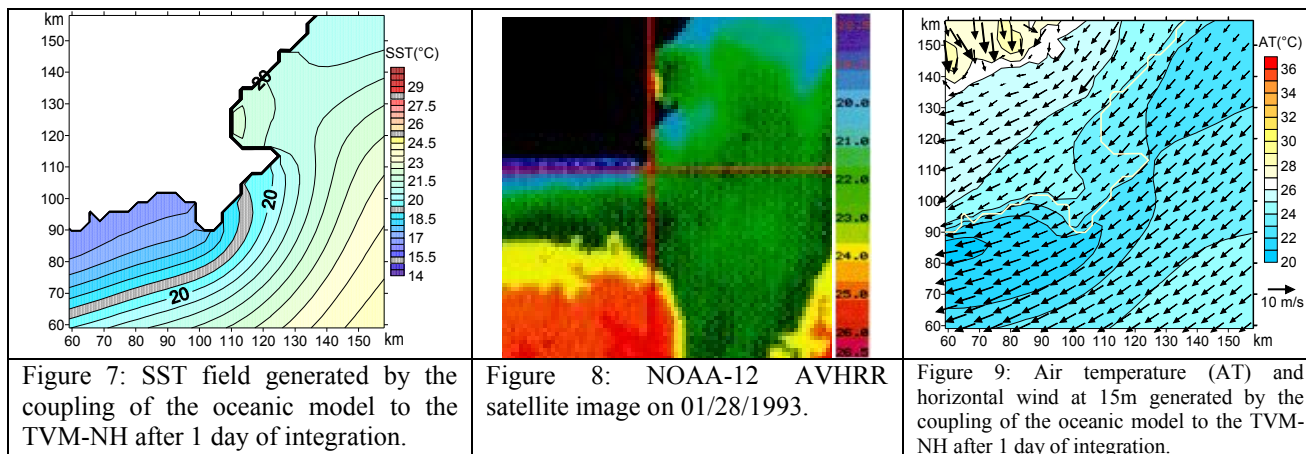


Figure 5: Domain and coastline considered by the model. Figure 6: The SST field after 2 days of integration of the oceanic model.

**Coupling:** Figure 7 shows the central part of the SST field generated by the oceanic model after one day of coupling and Figure 8 shows the SST satellite image. The two figures have a very similar SST field near the coastline, specially the cold water area west of the cape, where the coast is aligned in the E-W direction. The warmer water just north of the cape, where the coast is aligned is the N-S direction, appears in both figures, as well as the colder water at the upper right part of the domain, where the coastline is NE-SW. It is noticeable that the SST in Figure 7 is colder on the west part of the coastline and warmer on the northeast part of the coastline in comparison to Figure 6. It was caused by stronger winds over the west part of the coast and weaker winds over the northeast, showed on Figure 9.



## CONCLUSIONS

The oceanic model developed was able to represent very well important features of the SST field at the Cabo Frio area, specially the coastal upwelling phenomenon. It was also suitable for coupling to the TVM-NH atmospheric model and made possible the study of the interaction between the ocean and the atmosphere at this particular region. Future work will investigate the impact of the upwelling on the PBL and on the sea breeze circulation.

**AGRADECIMENTOS:** We thank the Brazilian Research Agency CNPq (grant 142007/2005-6) for funding this work. We also thank the support given by the Fundação de Amparo à Pesquisa do Estado de São Paulo (FAPESP).

## REFERÊNCIAS BIBLIOGRÁFICAS

- Carbonel, C. A. A. H. Modelling of upwelling-downwelling cycles caused by variable wind in a very sensitive coastal system. *Continental Shelf Research*, 23, 1559-1578, 2003.
- Clappier, A.; Martilli, A.; Grossi, P. et al. Effect of Sea Breeze on Air Pollution in the Greater Athens Area. Part I: numerical simulations and field observations. *J. Appl. Meteorology*. 39(4), 546-562, 2000.
- Dourado, M. S.; Oliveira, A.P. A numerical investigation of the atmosphere-ocean thermal contrast over the coastal upwelling region of Cabo Frio, Brazil, *Atmosfera*, 21(1), 13-34, 2008.
- Dourado, M. S.; Oliveira, A. P. Observational description of the atmospheric and oceanic boundary layer over the Atlantic Ocean. *Rev. Bras. Oceanogr.*, 49(1/2), 49-59, 2001.
- Franchito, S. H.; Rao, V. B.; Stech, J. L. et al. The effect of coastal upwelling on the sea-breeze circulation at Cabo Frio, Brazil: a numerical experiment. *Ann. Geophysicae*, 16, 866-881, 1998.
- Oda, T. O. Influencia da ressurgência costeira sobre a circulação local em Cabo Frio (RJ). São Paulo, 1997. 140p. Dissertação (Mestrado) – Programa de Pós-Graduação em Meteorologia, INPE.
- Orgaz, M.D.M.; Fortes, J.L. Estudo das brisas costeiras na região de Aveiro. In *Proceedings do 1º Simpósio de Meteorologia e Geofísica Hispano Português*. Lagos, Portugal. 1998.
- Stivari, S. M. S.; Oliveira, A. P.; Karam, Hugo A. et al. Patterns of Local Circulation in the Itaipu Lake Area: Numerical Simulations of Lake Breeze. *Journal of Applied Meteorology*. 42, 37 – 50, 2003.
- Thunis, P. Formulation and Evaluation of a Nonhydrostatic Vorticity Mesoscale Model. Belgium, 1995. 151p. Thesis (Ph.D) - Institut d'Astronomie et de Géophysique G. Lamaître, Université Catholique de Louvain, Louvain-la-Neuve.
- Verboom, G. K.; Slob, A. Weakly reflective boundary conditions for two-dimensional shallow water flow problems. Delft Laboratory. Publication n° 322, 1984.